한국동력기계공학회지 제13권 제4호 pp.49~55 2009년 8월

Three Dimensional Stress Analysis of Composite Laminates using Stress Functions and Interface Modeling
응력함수와 층간면 모델링을 이용한 복합재 적층판의 3차원 응력해석

H. S. Kim, J. Y. Kim and J. G. Kim
김흥수 · 김정윤 · 김진곤

(received 02 April 2009, revised 30 June 2009, accepted 22 July 2009)

주요 용어 : 층간응력(Interlaminar Stress), 자유단(Free Edge), 응력함수(Stress Function), 층간면 모델링(Interface Modeling), 응력특이(Stress Singularity)

요 약 : 복합재 적층판의 자유단 근처에서 나타나는 층간 응력의 집중 현상을 층간면 효과를 고려해 해석하였다. 복합재 적층판 내부의 임의의 위치에서 3차원 평형방정식을 만족시키기 위해 렉니츠키 응력함수를 도입하였으며, 가상일의 원리를 이용하여 지배방정식을 유도하였다. 주어진 응력함수를 이용하여 구한 3차원 응력들은 복합재 적층판의 아래 위 면뿐만 아니라 자유단에서 하중자유조건을 잘 만족한다. 기하학적 불연속성 때문에 복합재 적층판의 자유단에서는 응력의 특이가 발생하지만, 층간면 효과를 고려하게 되면 층간응력의 집중현상을 정확하게 해석할 수 있다. 자유단에서 발생한 층간응력의 크기를 보면, 층간면 효과를 고려할 경우, 응력특이 효과가 많이 줄어드는 것을 관찰할 수 있다. 본 연구에서 주어진 층간면에서의 정확한 응력 해석은 복합재 적층판의 강도설계를 수행하는 초기 설계 툴로 사용할 수 있다.

1. Introduction

Stress singularity and concentration generally occur in the free edges of composite laminates. The free edge stress initiates failure of the laminates. The interlaminar stresses are critical issues at the interfaces between layers near the free edges. Therefore, stress analysis near the free edges have been an important research topic for decades.

Most researchers assumed that each layer was homogeneous and anisotropic materials. The adjacent layers were also assumed as perfectly bonded. Linear elastic models and simple regular stress function-based approximation methods have been proposed in the previous studies[1-11]. However, the interlaminar stress singularity at the interface between dissimilar materials was recognized[12], and it became necessary to incorporate fracture mechanics approach to analyze the stresses near the free edges. The intensity of singularity depends on the material properties of the adjacent dissimilar materials. In reality, however, polymeric composite laminates have epoxy-resin interlayers between adjacent plies as shown in Fig. 1. Therefore, elasticity modeling with singular free-edge stresses is not appropriate in the prediction of the interlaminar stresses. Simple approximate analysis techniques have also been developed to obtain finite concentration stresses without singularities at the free edges[1-5]. The approximate stresses were finite but resulted from the assumption of regular basis functions. Thus, this kind of approximation could not provide the qualitatively correct behavior at the free edges within the assumed framework of linear elasticity. In the present study, the interface resin-rich epoxy interlayer modeling is considered. This modeling described

김흥수(책임저자):대구가톨릭대학교 기계자동차공학부
E-mail : heungsookim@cu.ac.kr, Tel : 053-850-2715
김정윤, 김진곤 : 대구가톨릭대학교 기계자동차공학부

the interface of laminates more realistically and the continuously varying material properties through the plies do not generate singular interlaminar stresses at the free edges.

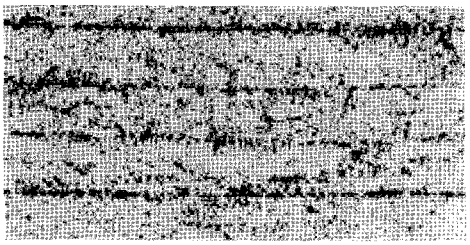

Fig. 1 Cross sectional SEM image of composite laminate

The objective of the present study is to investigate the effect of interface modeling on the interlaminar stresses and strength at the straight free edges. Symmetric cross-ply and angle-ply layups are analyzed. The failure strength is well predicted by the present model, which includes the reduction effect of peak values of interlaminar stress due to the epoxy resin layer between laminas.

2. Mathematical Formulation

The geometry of composite laminate with free edges is given in Fig. 2. The laminate consists of orthotropic materials. The thickness of each ply is equal and the plies have arbitrary angles relative to the x axis. Unidirectional extension is considered in the present study.

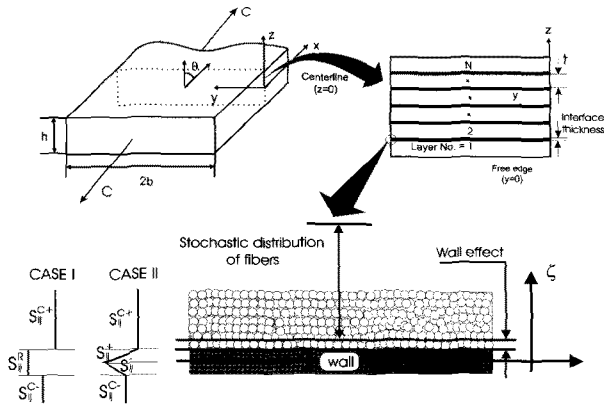

Fig. 2 Geometry of composite laminate with interface modeling

The linear elastic constitutive equations are assumed in each ply and they are expressed in the following form.

$$\begin{Bmatrix}\epsilon_1\\ \epsilon_2\\ \epsilon_3\\ \epsilon_4\\ \epsilon_5\\ \epsilon_6\end{Bmatrix}=\begin{bmatrix}S_{11} & S_{12} & S_{13} & 0 & 0 & S_{16}\\ S_{12} & S_{22} & S_{23} & 0 & 0 & S_{26}\\ S_{13} & S_{23} & S_{33} & 0 & 0 & S_{36}\\ 0 & 0 & 0 & S_{44} & S_{45} & 0\\ 0 & 0 & 0 & S_{45} & S_{55} & 0\\ S_{16} & S_{26} & S_{36} & 0 & 0 & S_{66}\end{bmatrix}\begin{Bmatrix}\sigma_1\\ \sigma_2\\ \sigma_3\\ \sigma_4\\ \sigma_5\\ \sigma_6\end{Bmatrix} \tag{1}$$

From the first row of Eq. (1), following relationship is obtained

$$\sigma_1 = (\epsilon_1 - S_{ij}\sigma_j)/S_{11} \quad (j = 2,3,6) \tag{2}$$

Substituting Eq. (2) into Eq. (1) leads to the strain components, which can be expressed as follows

$$\epsilon_i = \hat{S}_{ij}\sigma_j + \frac{S_{i1}}{S_{11}}\epsilon_1 \quad (i,j = 2,3,...6) \tag{3}$$

where

$$\hat{S}_{ij} = S_{ij} - S_{1i}S_{1j}/S_{11} \tag{4}$$

Compliance matrices of each layer are assumed to be homogeneous orthotropic materials. Two different compliance modelings for each interfaces are considered in the present study. CASE I is for constant resin compliance and ignores the wall effect as shown in Fig. 2. CASE II is for linearly varying compliance and considers the wall effect.

For CASE II, interface compliance is defined as follows.

$$\begin{aligned} S_{ij}^{+} &= (S_{ij}^{c+} - S_{ij}^{r})\zeta + S_{ij}^{r} \quad (0 < \zeta < 1)\\ S_{ij}^{-} &= -(S_{ij}^{c-} - S_{ij}^{r})\zeta + S_{ij}^{r} \quad (-1 < \zeta < 0) \end{aligned} \tag{5}$$

where ζ is local coordinate in z-direction at the interface. S_{ij}^{c+} represents upper layer compliance of the interface, S_{ij}^{c-} is lower layer compliance of the interface and S_{ij}^{r} is interface compliance.

For the given geometric configuration of laminates, traction free boundary conditions at

the free edge and the top and bottom surfaces must be satisfied as follows.

$$\begin{aligned}&\sigma_2=\sigma_4=\sigma_6=0 \quad at \quad y=0\\&\sigma_3=\sigma_4=\sigma_5=0 \quad at \quad z=\pm h/2\end{aligned} \tag{6}$$

Generalized plane strain states are assumed and the stress fields are independent of x-axis. Then, the displacement field can be written as follows

$$\begin{aligned}&u(x,y,z)=C\\&v(x,y,z)=V(y,z)\\&w(x,y,z)=W(y,z)\end{aligned} \tag{7}$$

where, C characterizes the stretch of the body along the x-axis and V(y,z) and W(y,z) represent its deformation in the y-z plane, respectively.

To make the problem simple, the coordinates are nondimensionalized as follows.

$$\eta=z/h,\ \xi=y/h \tag{8}$$

Lekhnitskii stress functions are introduced to satisfy pointwise equilibrium equations automatically[13]. These stress functions can be divided into the in-plane and out-of-plane functions.

$$\begin{aligned}&\frac{\partial^2 F}{\partial\eta^2}=\sigma_2,\ \frac{\partial^2 F}{\partial\xi^2}=\sigma_3,\ \frac{\partial^2 F}{\partial\eta\partial\xi}=-\sigma_4\\&\frac{\partial\Psi}{\partial\xi}=-\sigma_5,\ \frac{\partial\Psi}{\partial\eta}=-\sigma_6\end{aligned} \tag{9}$$

where

$$F=\sum_{i=1}^{n}f_i(\xi)g_i(\eta),\ \Psi=\sum_{i=1}^{n}p_i(\xi)g_i^I(\eta) \tag{10}$$

The superscript I in Eq.(10) denotes the differentiation with respect to η.

The governing equations are obtained by taking the principle of complementary virtual work.

$$\begin{aligned}0&=\iiint u_i\delta\sigma_{ij,j}dxdydz\\&=\iiint(u_i\delta\sigma_{ij}),_j-u_{i,j}\delta\sigma_{ij}dxdydz\\&=\iint_S u_i\delta\sigma_{ij}n_jdA\\&\quad-\iiint\frac{1}{2}(u_{i,j}+u_{j,i})\delta\sigma_{ij}dxdydz\end{aligned} \tag{11}$$

Using traction-free boundary conditions and neglecting rigid body motions, one obtains

$$\iint\triangle u\delta\sigma_{xx}dydz=\iint\epsilon_{ij}\delta\sigma_{ij}dydz \tag{12}$$

where

$$\triangle u=C \tag{13}$$

The in-plane stress functions are determined from the initially assumed basis set of out-of-plane stress functions. The out-of-plane functions must satisfy traction-free boundary conditions at the top and bottom surfaces (i.e. The stress functions and their first derivatives should be zero there). The out-of-plane functions are assumed to be the eigenmodes of a clamped-clamped beam. The stress functions $g_i(\eta)$ through the thickness are given as follows.

$$g_i(\eta)=\cos(k_i\eta)+\sigma_i\cosh(k_i\eta) \tag{14}$$

where, k_i's are the solutions of following characteristic equation.

$$\begin{aligned}&\cosh(k_i/2)\sin(k_i/2)\\&\qquad+\cos(k_i/2)\sinh(k_i/2)=0\\&\sigma_i=-\cos(k_i/2)/\cosh(k_i/2)\end{aligned} \tag{15}$$

Substituting Eq. (9) into Eq (12), the stresses are expressed in terms of f_i and p_i. Eq. (12) reduces to the following form after integration by parts.

$$\begin{aligned}&\int\left[a_{ij}^{(4)}f_j^{IV}+a_{ij}^{(2)}f_j^{II}+a_{ij}^{(0)}f_j\right.\\&\qquad\left.+b_{ij}^{(2)}p_j^{II}+b_{ij}^{(0)}p_j+ri\right]\delta f_id\xi\\&+\int\left[c_{ij}^{(2)}p_j^{II}+c_{ij}^{(0)}p_j\right.\\&\qquad\left.+d_{ij}^{(2)}f_j^{II}+d_{ij}^{(0)}f_j+si\right]\delta p_id\xi=0\\&\qquad(i,j=1,2,...,n)\end{aligned} \tag{16}$$

where

$$\begin{aligned}a_{ij}^{(4)}&=\int\hat{S}_{33}g_ig_jd\eta\\a_{ij}^{(2)}&=\int\hat{S}_{23}(g_i^{II}g_j+g_ig_j^{II})d\eta-\int\hat{S}_{44}g_i^Ig_j^Id\eta\\a_{ij}^{(0)}&=\int\hat{S}_{22}g_i^{II}g_j^{II}d\eta\end{aligned} \tag{17}$$

$$b_{ij}^{(2)} = \int \hat{S}_{36} g_i g_j^{II} d\eta - \int \hat{S}_{45} g_i^I g_j^I d\eta$$
$$b_{ij}^{(0)} = \int \hat{S}_{26} g_i^{II} g_j^{II} d\eta$$
$$c_{ij}^{(2)} = - \int \hat{S}_{55} g_i^I g_j^I d\eta$$
$$c_{ij}^{(0)} = \int \hat{S}_{66} g_i^{II} g_j d\eta$$
$$d_{ij}^{(2)} = \int \hat{S}_{36} g_i^{II} g_j d\eta - \int \hat{S}_{45} g_i^I g_j^I d\eta$$
$$d_{ij}^{(0)} = \int \hat{S}_{26} g_i^{II} g_j^{II} d\eta$$
$$r_i = \int \frac{S_{12}}{S_{11}} C g_i^{II} d\eta$$
$$s_i = \int \frac{S_{16}}{S_{11}} C g_i^{II} d\eta$$

The boundary terms induced by integration by parts are eliminated from the free edge boundary conditions such as $\sigma_2 = \sigma_4 = \sigma_6 = 0$.

In Eq. (16), the governing equations are reduced into the ordinary differential equations where $f_i(\xi)$ and $p_i(\xi)$ are coupled. The homogeneous solutions of f_i and p_i are assumed to be of following forms,

$$f_i = v_i^f e^{\lambda \xi},\ p_i = v_i^p e^{\lambda \xi} \tag{18}$$

Substituting Eq. (18) to Eq. (16), the ordinary differential equations are reduced to the following eigen system.

$$\begin{aligned} & a_{ij}^{(0)} v_j^f + (a_{ij}^{(2)} + \lambda^2 a_{ij}^{(4)})\, v_j^{f^{II}} \\ & \quad + (b_{ij}^{(0)} + \lambda^2 b_{ij}^{(2)}) v_j^p = 0 \\ & d_{ij}^{(0)} v_j^f + d_{ij}^{(2)} v_j^{f^{II}} + (c_{ij}^{(0)} + \lambda^2 c_{ij}^{(2)})\, v_j^p = 0 \\ & \lambda^2 v_j^f - v_j^{f^{II}} = 0 \qquad (i,j = 1,2,...,n) \end{aligned} \tag{19}$$

The 3rd equation of Eq. (19) is an auxiliary equation to convert the governing equation into an eigenproblem. Since the interlaminar stresses decay in the interior region of laminates, only the negative roots of λ^2 are selected. From the given eigenproblem, $3n$ eigenvalues are obtained, and the homogeneous solutions are obtained by $3n$ - term linear combinations as follows.

$$\begin{aligned} & f_i^{(H)} = v_{ij}^f t_j e^{-\lambda \xi} \\ & p_i^{(H)} = v_{ij}^p t_j e^{-\lambda \xi} \\ & (i = 1,2,...,n),\ (j = 1,2,...,3n) \end{aligned} \tag{20}$$

where t_j are constants to be determined from the boundary conditions.

The particular solutions can be obtained from the assumption that $f_i(\xi)$ and $p_i(\xi)$ in Eq. (16) are constants.

$$\begin{aligned} & a_{ij}^{(0)} f_j^{(P)} + b_{ij}^{(0)} p_j^{(P)} = - r_i \\ & b_{ij}^{(0)} f_j^{(P)} + c_{ij}^{(0)} p_j^{(P)} = - s_i \\ & \qquad (i,j = 1,2,...,n) \end{aligned} \tag{21}$$

Accordingly, the in-plane stress functions are expressed as the sum of the homogeneous and particular solutions.

$$\begin{aligned} & f_i = f_i^{(H)} + f_i^{(P)} \\ & p_i = p_i^{(H)} + p_i^{(P)}\ (i = 1,2,...,n) \end{aligned} \tag{22}$$

Calculation of t_j completes the determination of the in-plane functions. The coefficients t_j can be determined from the traction free boundary conditions of σ_2, σ_4, and σ_6 at the free edge.

$$\begin{aligned} & v_{ij}^f t_j = - f_i^{(P)} \\ & \lambda_j v_{ij}^f t_j = 0 \\ & v_{ij}^p t_j = - p_i^{(P)} \\ & \qquad (i = 1,2,...,n),\ (j = 1,2,...,3n) \end{aligned} \tag{23}$$

Substituting the calculated in-plane stress functions into Eq. (9), the interlaminar stresses can be obtained as follows.

$$\begin{aligned} \sigma_2 &= \left[v_{ij}^f t_j e^{-\lambda \xi} + f_i^{(P)} \right] g_i^{II}(\eta) \\ \sigma_3 &= \lambda_j^2 v_{ij}^f t_j e^{-\lambda \xi} g_i(\eta) \\ \sigma_4 &= \lambda_j v_{ij}^f t_j e^{-\lambda \xi} g_i^I(\eta) \\ \sigma_5 &= \lambda_j v_{ij}^p t_j e^{-\lambda \xi} g_i^I(\eta) \\ \sigma_6 &= \left[v_{ij}^p t_j e^{-\lambda \xi} + p_i^{(P)} \right] g_i^{II}(\eta) \\ & (i = 1, 2, ..., n),\ (j = 1, 2, ..., 3n) \end{aligned} \tag{24}$$

3. Numerical Results

For verification, composite laminates are analyzed for various layup configurations. The material properties of a ply are given as follows.

Laminates

$E_1 = 20 \times 10^6 psi,\ E_2 = E_3 = 2.1 \times 10^6 psi$

$G_{12} = G_{13} = G_{23} = 0.85 \times 10^6 psi$

$\nu_{12} = \nu_{13} = \nu_{23} = 0.21$

Epoxy

$E = 2.1 \times 10^6 psi,\ \nu = 0.21$

The in-plane length b is assumed to be $2h$. The in-plane and out-of-plane stress distributions are obtained, respectively, and they are compared with the previous results.

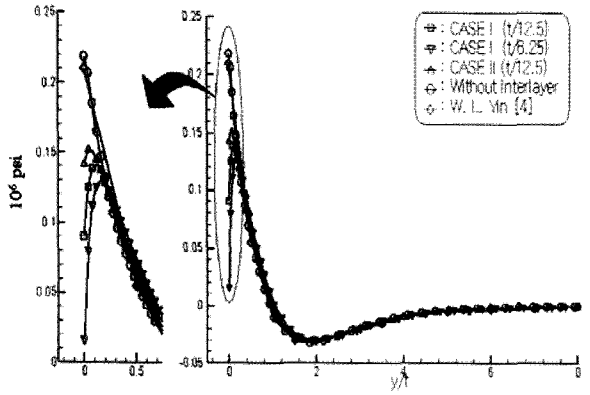

Fig. 3 σ_3 at the 0/90 interface of [0/90]s laminate

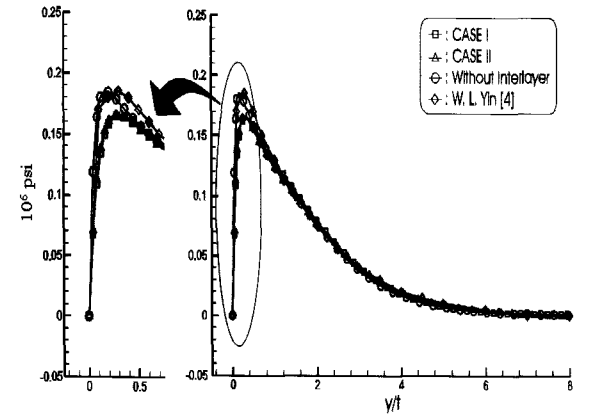

Fig. 4 σ_4 at the 0/90 interface of [0/90]s laminate

Fig. 3 shows the σ_3 distribution at 0/90 interface of $[0/90]_S$ laminate under unit extension. X-axis of the figure represents normalized in-plane coordinate (y-coordinate) by the ply thickness as shown in Fig. 2. Y-axis represents the magnitude of interlaminar normal stress. Interface interlayer modeling results in the reduction of peak interlaminar stresses. Stress distribution without interlayers agrees well with that of Yin[4]. The free-edge peak stresses decrease as the interface thickness increases. The peak stress of CASE I(constant interlayer compliances) is smaller than that of CASE II(linearly varying interlayer compliances). The interface thickness is assumed as $t/12.5$ for the rest of computations.

Fig. 4 shows the interlaminar shear stress distribution at the 0/90 interface of $[0/90]_S$ laminate under unit extension. The peak stresses with interface modeling decrease. CASE I and CASE II do not show the significant discrepancy.

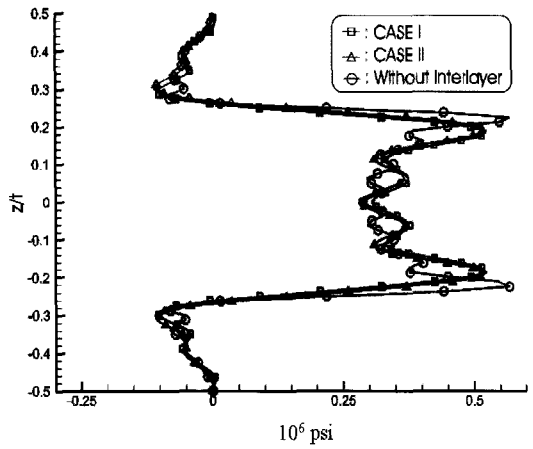

Fig. 5 σ_3 at the free edge of [0/90]s laminate

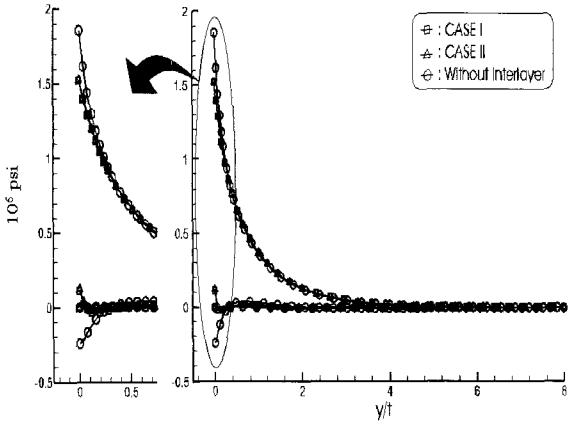

Fig. 6 $\sigma_3, \sigma_4, \sigma_5$ at the 45/-45 interface of [45/-45]s laminate

Fig. 5 depicts the interlaminar normal stress distribution at the free edge of $[0/90]_S$ laminate under unit extension. While the stress distribution without interlayer shows big jump at the interface, stresses predicted by interface modeling provides relatively smooth distribution through the thickness. There are only small discrepancy between CASE I and CASE II. Maximum stresses decrease significantly by considering the

interlayer effect.

Fig. 6 shows σ_3, σ_4, and σ_5 distribution at $45/-45$ interface of $[45/-45]_S$ laminate under unit extension. Y-axis of the figure represents normalized out-of-plane coordinate (z-coordinate) by the ply thickness as shown in Fig. 2. X-axis represents the magnitude of interlaminar normal stress. The interlaminar shear stress is dominant in this case and it has the same tendency as shown in cross-ply.

4. Conclusions

The interlaminar stresses near free edges in composite laminates considering interlayer modeling have been analyzed for unit extensional loading condition. The peak stresses are significantly reduced by introducing interface interlayer modeling. If the layers are considered as dissimilar anisotropic elastic materials, the free edge elasticity analysis provides singular interlaminar stresses. However, realistic interface modeling does not provide singular stresses at the free edges. This modeling provides only concentrated finite interlaminar stresses. Within this modeling, regular stress basis functions are legitimate for stress expression. The present approximate elasticity solutions provide finite stresses and they are consistent with the present interlayer modeling. Thus the present modeling avoids singular interlaminar stresses at the free edges and provides exact interlaminar strength of laminated composites. It is expected that the proposed interlayer modeling can be used as an efficient design tool in the initial design stage of laminated composite structures.

Reference

1. R. L. Spilker and S. C. Chou, 1980, "Edge Effects in Symmetric Composite Laminates : Importance of Satisfying the Traction-Free-Edge Condition", Journal of Composite Materials, Vol. 14, pp. 2~20.
2. C. Kassapoglou and P. A. Lagace, 1986, "An Effcient Method for the Calculation of Interlaminar Stresses in Composite Materials", Journal of Applied Mechanics, Vol. 53, pp. 744~750.
3. W. L. Yin, 1994, "Free-Edge Effects in Anisotropic Laminates Under Extension, Bending and Twisting. Part 1-A Stress Function Based Variational Approach", Journal of Applied Mechanics, Vol. 61, pp. 410~415.
4. W. L. Yin, 1994, "Free-Edge Effects in Anisotropic Laminates Under Extension, Bending and Twisting. Part 2-Eigenfunction Analysis and the Results for Symmetric Laminates", Journal of Applied Mechanics, Vol. 61, pp. 416~421.
5. T. Kim and S. N. Atluri, 1995, "Analysis of Edge Stresses in Composite Laminates Under Combined Thermo-Mechanical Loading, Using a Complementary Energy Approach", Computational Mechanics, Vol. 16, pp. 83~97.
6. G. Flanagan, 1994, "An Efficient Stress Function Approximation for the Free-Edge Stresses in Laminates", International Journal of Solids and Structures, Vol. 31, pp. 941~952.
7. M. Cho and J. Yoon, 1999, "Free-edge interlaminar stress analysis in composite laminates by the extended Kantorovich method", AIAA Journal, Vol. 37, No. 5, pp. 656~660.
8. M. Cho and H. S. Kim, 2000, "Iterative Free-Edge Stress Analysis of Composite Laminates under Extension, Bending, Twisting and Thermal Loadings". International Journal of Solids and Structures, Vol. 37, No. 3, pp. 435~459.
9. H. S. Kim, M. Cho and G. I. Kim, 2000, "Free-edge strength analysis in composite laminates by the extended Kantorovich method". Composite structure, Vol. 49, No. 2, pp. 229~235.
10. S. Y. Rhee, M. Cho and H. S. Kim, 2006, "Layup optimization with GA for tapered laminates with internal plydrops", International

Journal of Solids and Structures, Vol. 43, No. 16, pp. 4757~4776.

11. H. S. Kim, S. Y. Rhee and M. Cho, 2008, "Simple and Efficient Interlaminar Stress Analysis of Composite Laminates with Internal Ply-Drop", Composite Structures, Vol. 84, No. 1, pp. 73~86.
12. S. S. Wang and I. Choi, 1982, "Boundary Layer Effects in Composite Laminates Part 2 -Free Edge Stress Solutions and Basic Characteristics", Journal of Applied Mechanics, Vol. 49, pp. 549~560.
13. S. G. Lekhnitskii, 1963, "Theory of Elasticity of an Anisotropic Body", Holden-Day Inc., San Francisco.